

RESEARCH ARTICLE

Identification of Driving *ALK* Fusion Genes and Genomic Landscape of Medullary Thyroid Cancer

Jun Ho Ji¹✉, Young Lyun Oh²✉, Mineui Hong²✉, Jae Won Yun³, Hyun-Woo Lee², DeokGeun Kim⁴, Yongick Ji⁴, Duk-Hwan Kim⁴, Woong-Yang Park³, Hyun-Tae Shin³, Kyoung-Mee Kim², Myung-Ju Ahn⁵, Keunchil Park⁵, Jong-Mu Sun⁵*

1 Division of Hematology and Oncology, Department of Medicine, Samsung Changwon Hospital, Sungkyunkwan University School of Medicine, Changwon, Korea, **2** Department of Pathology and Translational Genomics, Samsung Medical Center, Sungkyunkwan University School of Medicine, Seoul, Korea, **3** Samsung Genome Institute, Samsung Medical Center, Seoul, Korea; Department of Molecular Cell Biology, Sungkyunkwan University School of Medicine, Suwon, Korea, **4** Molecular Translational Research Center, Samsung Biomedical Research Institute, Seoul, Korea, **5** Division of Hematology and Oncology, Department of Medicine, Samsung Medical Center, Sungkyunkwan University School of Medicine, Seoul, Korea

✉ These authors contributed equally to this work.

* tntntn3@gmail.com



 OPEN ACCESS

Citation: Ji JH, Oh YL, Hong M, Yun JW, Lee H-W, Kim D, et al. (2015) Identification of Driving *ALK* Fusion Genes and Genomic Landscape of Medullary Thyroid Cancer. *PLoS Genet* 11(8): e1005467. doi:10.1371/journal.pgen.1005467

Editor: Yuri E. Nikiforov, University of Cincinnati College of Medicine, UNITED STATES

Received: April 10, 2015

Accepted: July 24, 2015

Published: August 21, 2015

Copyright: © 2015 Ji et al. This is an open access article distributed under the terms of the [Creative Commons Attribution License](https://creativecommons.org/licenses/by/4.0/), which permits unrestricted use, distribution, and reproduction in any medium, provided the original author and source are credited.

Data Availability Statement: All relevant data are within the paper and its Supporting information files.

Funding: The authors received no specific funding for this work.

Competing Interests: The authors have declared that no competing interest exist.

Abstract

The genetic landscape of medullary thyroid cancer (MTC) is not yet fully understood, although some oncogenic mutations have been identified. To explore genetic profiles of MTCs, formalin-fixed, paraffin-embedded tumor tissues from MTC patients were assayed on the Ion AmpliSeq Cancer Panel v2. Eighty-four sporadic MTC samples and 36 paired normal thyroid tissues were successfully sequenced. We discovered 101 hotspot mutations in 18 genes in the 84 MTC tissue samples. The most common mutation was in the ret proto-oncogene, which occurred in 47 cases followed by mutations in genes encoding Harvey rat sarcoma viral oncogene homolog (N = 14), serine/threonine kinase 11 (N = 11), v-kit Hardy-Zuckerman 4 feline sarcoma viral oncogene homolog (N = 6), mutL homolog 1 (N = 4), Kiesten rat sarcoma viral oncogene homolog (N = 3) and MET proto-oncogene (N = 3). We also evaluated anaplastic lymphoma kinase (*ALK*) rearrangement by immunohistochemistry and break-apart fluorescence *in situ* hybridization (FISH). Two of 98 screened cases were positive for *ALK* FISH. To identify the genomic breakpoint and 5' fusion partner of *ALK*, customized targeted cancer panel sequencing was performed using DNA from tumor samples of the two patients. Glutamine:fructose-6-phosphate transaminase 1 (*GFPT1*)-*ALK* and echinoderm microtubule-associated protein-like 4 (*EML4*)-*ALK* fusions were identified. Additional PCR analysis, followed by Sanger sequencing, confirmed the *GFPT1*-*ALK* fusion, indicating that the fusion is a result of intra-chromosomal translocation or deletion. Notably, a metastatic MTC case harboring the *EML4*-*ALK* fusion showed a dramatic response to an *ALK* inhibitor, crizotinib. In conclusion, we found several genetic mutations in MTC and are the first to identify *ALK* fusions in MTC. Our results suggest that the *EML4*-*ALK* fusion in MTC may be a potential driver mutation and a valid target

of *ALK* inhibitors. Furthermore, the *GFPT1-ALK* fusion may be a potential candidate for molecular target therapy.

Author Summary

Little is known about the molecular biology of medullary thyroid cancer (MTC), which is a rare disease. Genomics are increasingly being used to improve our knowledge about disease biology and to identify therapeutic targets in many cancers. Here, we report the largest genomic results of MTC to date. MTC tissue frequently included several mutations. For the first time, anaplastic lymphoma kinase (*ALK*) rearrangements were detected in MTC: one case with a glutamine:fructose-6-phosphate transaminase 1 (*GFPT1-ALK*) fusion, and another case with an echinoderm microtubule-associated protein-like 4 (*EML4-ALK*) fusion. The fusion mechanism of the novel *GFPT1-ALK* fusion was successfully investigated using molecular biology techniques. In addition, an inhibitor of *ALK* (crizotinib) dramatically decreased the number of metastatic MTC lesions harboring the *EML4-ALK* fusion, thus verifying the fusion as a promising target in MTC. Our findings suggest that using rapidly improving sequencing techniques and accumulated genomic data to comprehensively perform genetic analyses on rare tumors, such as MTC, will help to improve the poor prognosis of orphan diseases.

Introduction

Many cancer gene profiling studies have recently been published, describing genetic trends that are not limited to specific cancers. Next-generation sequencing (NGS) is an important tool for detecting genetic alterations in many kinds of cancers, as it allows for millions of nucleic acid sequences to be simultaneously sequenced within a short period of time and is more cost-effective than older methods. Thus, many researchers and physicians anticipate that NGS will bring the concept of personalized cancer therapy to fruition.

Medullary thyroid cancer (MTC) is a rare malignancy that accounts for up to 3–5% of thyroid cancers. It is derived from calcitonin-secreting para-follicular C cells and can arise in a familial (25%) or sporadic (75%) pattern. Genetic and epigenetic alterations play important roles in the progression and prognosis of MTC [1–3]. Genes encoding the ret proto-oncogene (*RET*) and Ras (*RAS*) are commonly mutated in MTC [4, 5]. The *RET* mutation is believed to be a causative event in both familial and sporadic MTC [6, 7]. In the Mitogen-activated protein kinase (MAPK) pathway, the *RAS* mutation is another genetic rearrangement that is prevalent in sporadic MTC and other types of thyroid cancer [2] but the prevalence and significance of other genetic mutations including *BRAF* in MTC remain unclear.

MTC has a different response to treatment than that of well-differentiated thyroid cancers. Because radioactive iodine does not accumulate in MTC, few therapeutic options are available for advanced MTC. Inhibitors of *RET*, such as cabozantinib and vandetanib, have recently been shown to be effective in advanced MTC [8, 9]. However, whether the *RET* mutation is a predictive factor for the success of these drugs is unclear [9].

Recently, the rearrangement of anaplastic lymphoma kinase (*ALK*) was detected in a small but significant proportion of patients with non-small cell lung cancer (NSCLC) [10]. Several *ALK* inhibitors, including crizotinib, have achieved dramatic responses in cases of NSCLC harboring *ALK* rearrangements [11–13]. Although *ALK* rearrangement has also been episodically

Table 1. Demographic, pathologic and genetic characteristics of medullary thyroid cancer patients.

	Amino acid change in <i>RET</i>		Stage (AJCC 7 th)		Age (min-max)/ Gender
Hereditary MTC (11)	C634Y	3	I	4	35.3 (20–57)
	C634W	4	II	0	M:F 5:6
	D631Y	2	III	5	
	C634G	2	IV	2	
		11 (100%)	N/A	0	
Sporadic MTC (41)	M918T	15	I	9	50.3 (22–74)
	Deletion	4	II	4	M:F 19:22
	C630R	2	III	6	
	C634R	1	IV	21	
	C634Y	1	N/A	1	
	C618S	1			
	A883V	1			
	25 (61.0%)				
Unknown (32)	M918T	4	I	18	50.6 (17–76)
	C634Y	3	II	3	M:F 8:24
	C630R	2	III	4	
	C634G	2	IV	5	
		11 (34.3%)	N/A	2	

doi:10.1371/journal.pgen.1005467.t001

observed in a small set of other cancer types, little is known about *ALK* rearrangements in MTC [14, 15].

In this study, we used targeted NGS and various methods to examine the genetic profiles of MTC and detect *ALK* rearrangements.

Results

Basal characteristics and prevalence of gene mutations that are detected by AmpliSeq

Eighty-four samples (11 hereditary, 41 sporadic and 32 unknown) from patients with MTC (mean age of 48.5 years) and 36 paired normal thyroid tissue samples were successfully sequenced. The normal thyroid tissue samples in the MTC patients were used as matched control samples. Of the cases, 32 were male and 52 were female. Detailed demographic, clinic-pathological and genetic characteristics are listed in Table 1 and S2 Table. Hereditary MTCs were defined as cases having either positive germ-line *RET* mutations in blood tests or possession of a strong family history with MTC in at least four family members [16]. The unknown group was composed of MTC cases with no blood *RET* test and no family history of MTC/MEN. The mean value of variant coverage was 593 reads, and the variant coverage ranged from 19 to 1,482 reads. Overall, 101 mutations were observed in the MTC samples. Most mutations (N = 96, 95.0%) were single-nucleotide variants; 5 were deletions. The most common mutation occurred in *RET*, which was observed in 47 cases, followed by mutations in genes encoding Harvey rat sarcoma viral oncogene homolog (N = 14), serine/threonine kinase 11 (N = 11), v-kit Hardy-Zuckerman 4 feline sarcoma viral oncogene homolog (N = 6), *mutL* homolog 1 (N = 4), Kiesten rat sarcoma viral oncogene homolog (N = 3), *MET* proto-oncogene (N = 3), *ATM* serine/threonine kinase (N = 2), kinase insert domain receptor (N = 2), adenomatous polyposis coli (*APC*; N = 2), *B-raf* proto-oncogene (N = 1), *cadherin 1* (N = 1),

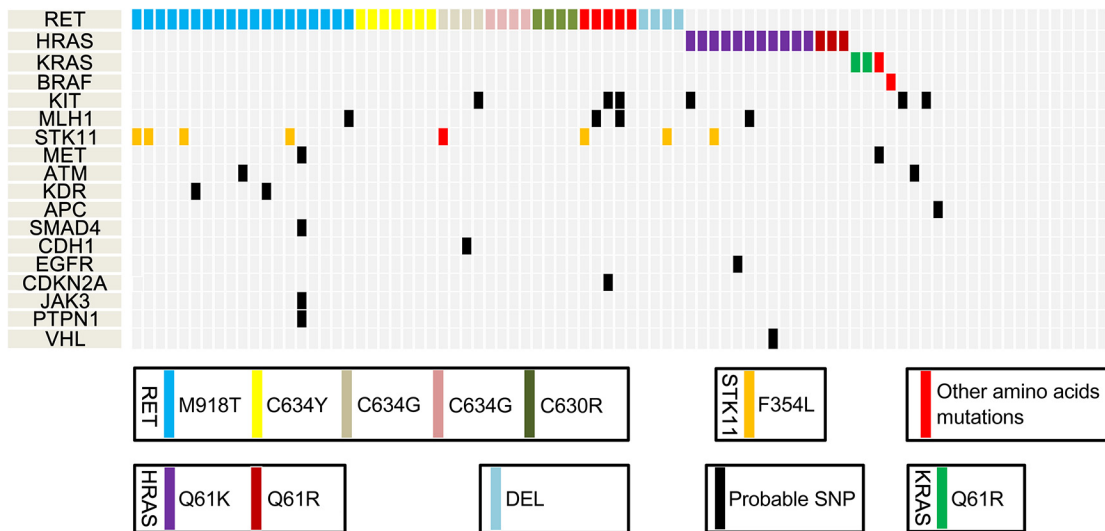


Fig 1. Mutational profiles of medullary thyroid cancer (MTC), as identified by next-generation sequencing. SNP, single-nucleotide polymorphism; DEL, deletion.

doi:10.1371/journal.pgen.1005467.g001

epidermal growth factor receptor (N = 1), cyclin-dependent kinase inhibitor 2A (*CDKN2A*, N = 1), Janus kinase 3 (N = 1), protein tyrosine phosphatase, non-receptor type 1 (N = 1), SMAD family member 4 (N = 1) and von Hippel-Lundau tumor suppressor (N = 1). We did not detect any dominant gene mutations in 20 MTC samples, which all exhibited wild-type *RET*, *HRAS* and *KRAS*. These are listed in [S1 Table](#) and shown in [Fig 1](#).

Specific types of gene mutations

The commonly observed *RET* mutations occurred in exons 10, 11, 15, and 16. Previous studies have shown that M918T is the most common *RET* mutation in MTC [2, 10]. Similarly, M918T (N = 19) was the most common *RET* mutation in our samples, followed by C634Y (N = 7), C634W (N = 4), C634G (N = 4), C630R (N = 4), D631Y (N = 2), and others (N = 7). All *HRAS* mutations occurred in exon 3. The mutant amino acid sequence in each of the *HRAS* mutant cases was Q61K (N = 13). *KRAS* mutations were observed in three cases (Q61R, 2 and G48R, 1), and *BRAF* mutation was found in only one case. The dominant amino acid sequence in *STK11* was F354L (N = 7). Other mutated genes are shown in [S1 Table](#).

Comparative analysis between MTC tissue and matched normal thyroid tissue

We compared the genetic landscapes between 36 MTC tissues and their matched normal thyroid tissues: this group was composed of 16 sporadic, 5 hereditary and 15 cases with unknown information about heredity ([Fig 2](#)). In the hereditary MTC cases, *RET* mutations were observed in MTC and their matched normal thyroid tissues: these *RET* mutation types included C634Y, D631Y, and C634W, which are well known to be associated with the MEN2A [17, 18]. One case, which had been classified as an unknown subgroup based on blood test or family history, was found to have C634W mutation in both MTC and normal tissue, leading us to suspect that this case might be hereditary MTC. In 16 sporadic MTC group, several *RET* mutation types (M918T, C630R, C618S and deletion) were detected in MTC tissues, but not in the matched normal thyroid tissues. The M918T *RET* mutations and Q61K *HRAS* mutations were observed only in the MTCs of the sporadic or unknown subgroups, suggesting that these mutations are

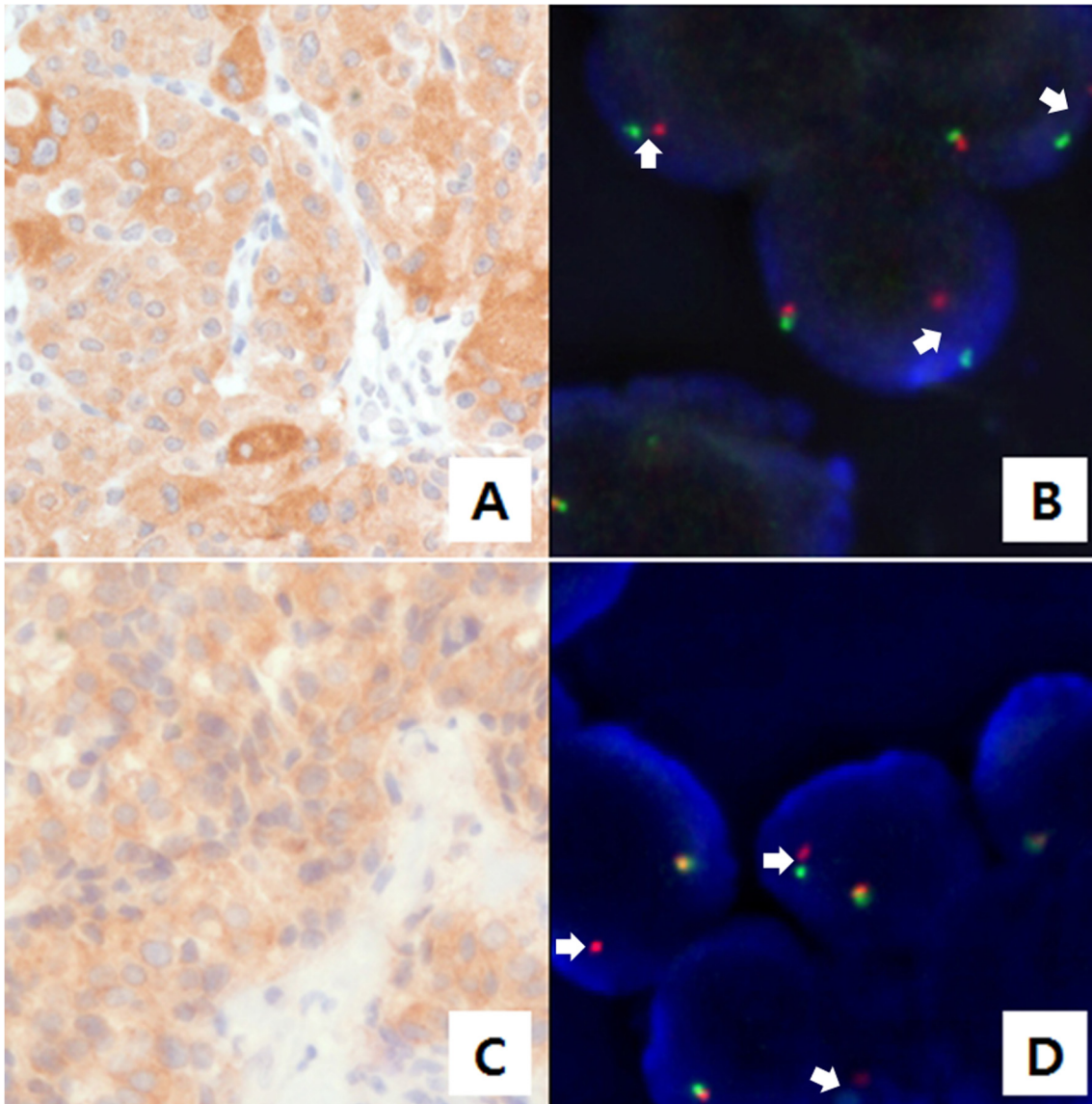


Fig 3. Anaplastic lymphoma kinase (ALK) staining using immunohistochemistry (IHC) and fluorescence *in situ* hybridization (FISH). (A) and (C) ALK staining in tumor cells was detected by IHC. (B) and (D) Results of FISH with the break-apart *ALK* probe are shown. A single red signal or splitting of the red and green signals was observed (marked with arrows). The cases shown in A/B and C/D exhibited glutamine:fructose-6-phosphate transaminase 1 (*GFPT1*)-*ALK* and echinoderm microtubule-associated protein-like 4 (*EML4*)-*ALK* fusions, respectively.

doi:10.1371/journal.pgen.1005467.g003

intra-chromosomal translocation or deletion. To confirm the fusion, we amplified the genomic fusion point between *GFPT1* and *ALK* using genomic DNA of the MTC tissue. PCR analysis and Sanger sequencing revealed the same results as that of the customized targeted cancer panel (Figs 4B and S1). For the second case, the echinoderm microtubule-associated protein-like 4 (*EML4*)-*ALK* fusion was detected. The breakpoints were located in intron 13 of *EML4* and intron 19 of *ALK*, which indicates that this fusion is the most common variant (E13; A20) in NSCLC [19, 20]. This case exhibited metastatic lesions after thyroidectomy and was enrolled in a Phase I crizotinib trial (NCT01121588). After crizotinib therapy, the tumor lesions in the lung, liver, and bone shrank remarkably, and plasma calcitonin levels decreased. The final results will be disclosed with the full clinical study.

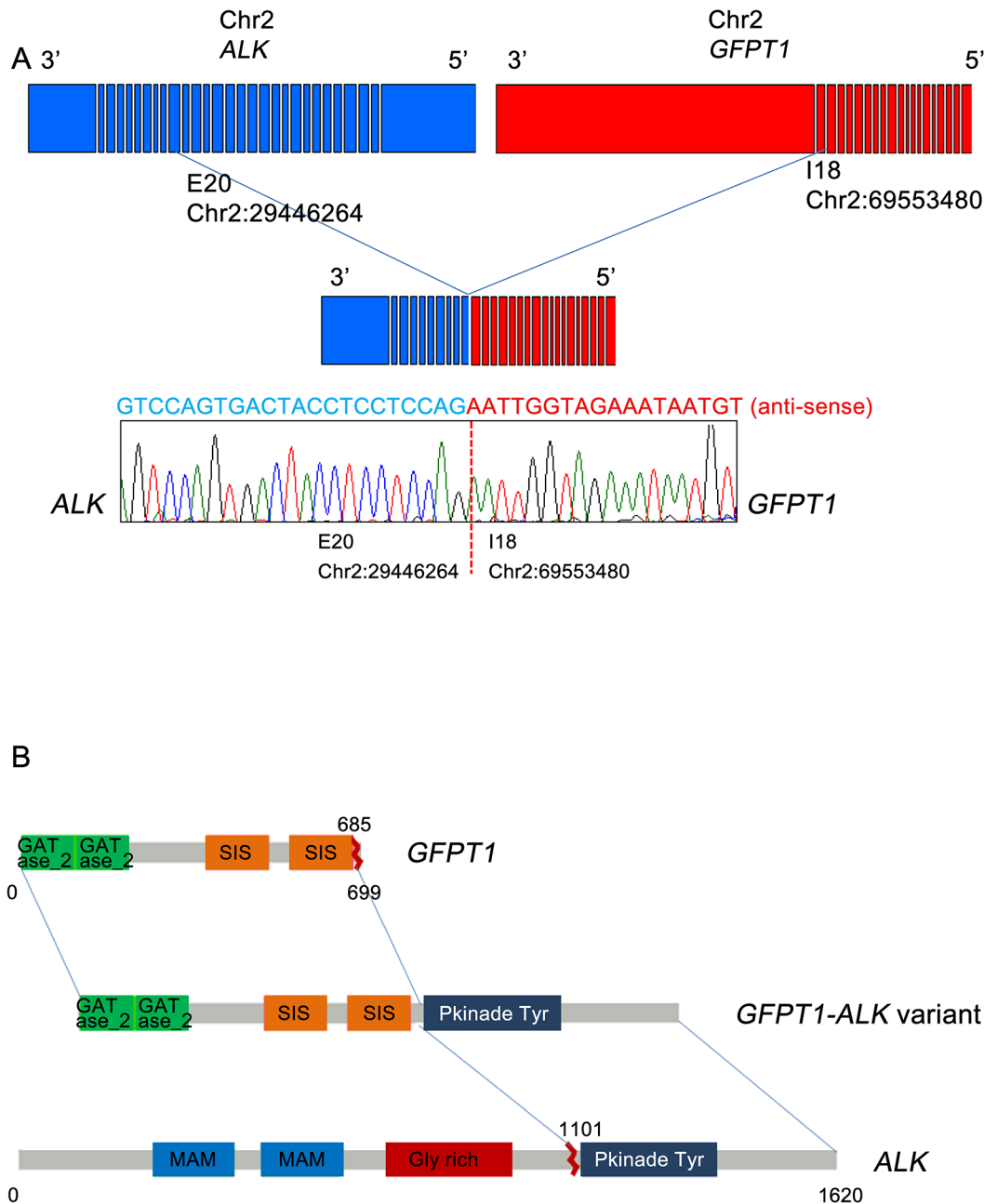


Fig 4. Gene fusion between *GFPT1* and *ALK*. (A) Schematic representation of the fusion of the 5' *GFPT1* to 3' *ALK*. (B) The fusion of *GFPT1* to *ALK* is oriented in the same direction and is located in 2p23. Confirmation of the *GFPT1-ALK* fusion was carried out by reverse transcription-polymerase chain reaction and Sanger sequencing. GATase_2, glutamine aminotransferases class-II; SIS, Sugar ISomerase domain; MAM, meprin/A5-protein/PTPmu domain; Gly_rich, glycine rich protein; Pkinase_Tyr, protein tyrosine kinase.

doi:10.1371/journal.pgen.1005467.g004

Discussion

We identified two types of *ALK* fusion genes in MTC by sequencing via IHC, FISH, and NGS analyses. Of the two fusion types, the *EML4-ALK* fusion was the same as the most commonly detected variant in NSCLC, [19] where the *EML4-ALK* fusion is a strong predictive factor for the efficacy of *ALK* inhibitors [13, 21, 22]. In the current study, the patient with metastatic MTC harboring the *EML4-ALK* fusion showed a dramatic response to crizotinib. We are the

first to report an MTC case with a targetable *EML4-ALK* fusion gene. Previously, Kelly et al. used the Illumina HiSeq sequencing system to identify one papillary thyroid cancer case with an *EML4-ALK* fusion [15]. However, they also tested 22 medullary carcinoma cases and did not find any cases with the *EML4-ALK* fusion, as evaluated by reverse transcription-PCR. Their failure to detect the *ALK* rearrangement in MTC is understandable, given that our prevalence rate of *ALK* fusions in the current study was only 2% (2 out of 98 cases). This suggests that more efficient strategies are needed to detect the *ALK* rearrangement. Results from the current study suggest that IHC-based screening, along with FISH-based confirmation and targeted NGS, may be a cost-effective and reliable method to detect *ALK* rearrangements.

Most importantly, we detected a novel *GFPT1-ALK* fusion that has not been reported in any type of cancer. *GFPT1* is a key enzyme in the biosynthesis of N-acetylglucosamine and is required for critical events in neuromuscular transmission [23]. Until now, several fusion partners of *ALK* have been reported in various cancers [24–28]. Among them, huntingdon-interacting protein (*HIP1*)-*ALK* and RAN-binding protein 2 (*RANBP2*)-*ALK*, which have been reported to exist in NSCLC and inflammatory myofibroblastic tumors, respectively, show clinical responses to crizotinib [25, 26]. In the current study, the MTC case harboring the *GFPT1-ALK* fusion showed strong *ALK* protein expression and did not exhibit co-existing genetic mutations; both of these factors may support an important role for this fusion gene in the pathogenesis of this MTC case. However, we were unable to validate whether *GFPT1-ALK* was a driving oncogene or a therapeutically targetable gene. Whether *GFPT1-ALK* is also a predictor for *ALK* inhibitors is unclear.

Currently, vandetanib and cabozantinib are approved for the treatment of MTC by the U.S. Food and Drug Administration. However, the prognosis of patients with metastatic MTC is still poor, due to the inherent resistance to radioiodine therapy and aggressive nature of this disease. Furthermore, the rarity of MTC makes it hard to perform prospective studies to find new agents. Therefore, the comprehensive genetic analysis of MTC can help to identify effective ways to improve its prognosis. Despite the low frequency of *ALK* rearrangements in MTC, our techniques can be used to detect target genes in other rare diseases.

In addition, our sequencing analysis of MTC is the largest to date. Previously, Agrawal et al. published the largest genomic analysis of MTC [5], where they performed whole-exome sequencing of 17 sporadic MTCs and 40 additional MTCs (hereditary or sporadic) for validation. *RET* was the dominant mutation (43/57) in that study. We used a larger sample size and accurate verification by comparing 36 pairs of MTC with matched normal thyroid tissues that were acquired from the same person.

In the comparison analyses, all five hereditary cases were observed to have germ-line *RET* mutations in both MTC and control tissues. However, M918T *RET* (N = 10), Q61K *HRAS* (N = 7), *KRAS* (N = 2), and *MET* (N = 1) mutations were harbored dominantly in MTCs. Simbolo et al. identified *RET*, *HRAS*, *KRAS* and *STK11* mutations as significant somatic mutations in MTCs, whereas *TP53*, *KDR*, *KIT*, *MET*, *PIK3CA* and *ATM* mutations were classified as non-pathogenic germ-line variants [29]. Our current data are compatible with that report. Interestingly, however, the F354L *STK11* mutation, regarded as significant somatic mutation by Simbolo et al., was observed in both MTCs and control tissues of our seven cases. Therefore, we presume that the F354L *STK11* mutation is a germ-line mutation in MTC.

In conclusion, we report that the *EML4-ALK* fusion, which was found for the first time in MTC, could be an effective molecular target of crizotinib. Furthermore, our results also suggest that the novel *GFPT1-ALK* fusion can be a potential candidate for molecular target therapy. This study included the largest set of molecular profile data in MTC to date, which was achieved by using high-depth NGS panel sequencing, and also presented the genetic landscape

of MTC. Further translational research is needed to determine the oncogenic roles of these mutations in MTC.

Materials and Methods

Ethics statement

Written informed consent was obtained from all participants, and this study was approved by the Institutional Review Board of Samsung Medical Center. (SMC 2013-02-010).

Searching for genetic mutation profiles by Ampliseq

We collected data on patients who were histologically diagnosed with MTC without the coexistence of tumors on the parathyroid and adrenal gland. All patients received surgical treatment at Samsung Medical Center between June 2000 and January 2013. Among 101 MTC specimens, 17 were excluded based on quality control ($N = 5$), preparation failure ($N = 11$), and sequencing failure ($N = 1$). The remaining 84 MTC samples were sequenced using an Ion Torrent Personal Genome Machine (IT-PGM, Life Technologies, Grand Island, NY, USA), which takes real-time measurements of hydrogen ions that are produced during DNA replication and allows for rapid sequencing. Eight normal thyroid tissues were obtained by thyroidectomy and sequenced. Mutation profiles between MTC and normal thyroid tissues from eight individuals were compared.

We constructed libraries using the Ion AmpliSeq Panels, Ion AmpliSeq Library Kit, and Ion Xpress Barcodes, as well as 10 ng of DNA sample per pool (Life Technologies). The amplicons were ligated to Ion Adapters and purified. For barcoded library preparations, barcoded adapters from the Ion Xpress Barcode Adapters 1–96 Kit were substituted for the non-barcoded adapter mix in the Ion AmpliSeq Library Kit. Next, the multiplexed barcoded libraries were enriched by clonal amplification using emulsion polymerase chain reaction (PCR) on Ion Sphere Particles (Ion PGM Template 200 Kit) and loaded on an Ion 316 Chip. Massively parallel sequencing was carried out on an Ion PGM using the Ion PGM Sequencing 200 Kit v2. The Ion AmpliSeq Cancer Hotspot Panel v2 covered hotspot regions of 50 oncogenes and tumor suppressor genes.

The primary filtering process was performed with the Torrent Suite v4.0.0 and Ion Torrent Variant Caller v4.0 software and included signal processing, base calling, assigning quality scores, adapter trimming, PCR duplicate removal, read alignment (to human genome reference 19), mapping quality control, coverage analyzing, and variant calling [30]. To detect variants, a minimum coverage of 100 reads was achieved with a cutoff value of at least 5% in the variant calling rate (frequency). Variant calls were further analyzed by using ANNOVAR variant filtering and COSMIC database (dbSNP build 137) annotating, and these analyses were based on changes in the amino acid sequence.

ALK immunohistochemistry (IHC) and fluorescence *in situ* hybridization (FISH)

The *ALK* IHC assay used a mouse monoclonal *ALK* antibody (5A4, Novocastra, Newcastle, United Kingdom) and the antibody for *ALK* was diluted to 1:30, treated, and incubated at 42°C for 2 hours. *ALK* IHC scores were assigned as follows: 0, no staining; 1+, faint or weak staining intensity with more than 5% tumor cells or any staining intensity with $\leq 5\%$ tumor cells; 2+, moderate cytoplasmic reactivity with more than 5% tumor cells; and 3+, granular cytoplasmic reactivity of strong intensity in more than 5% of tumor cells [31]. Cases that showed *ALK*-positive staining with a score of 1+ or greater were analyzed by FISH with the Vysis *ALK* Break-Apart FISH Probe Kit (Abbott Laboratories, Abbott Park, IL). Samples were considered

positive for *ALK* FISH if more than 15% of cells were positive or an isolated red signal (IRS) in tumor cells.

Customized targeted cancer panel sequencing for *ALK* fusion genes

Genomic DNA extraction was performed using the QIAamp DNA mini kit (Qiagen, Valencia, CA, USA), according to the manufacturer's instructions. The Nanodrop 8000 UV-Vis spectrometer (Thermo Scientific Inc., DE, USA), Qubit 2.0 Fluorometer (Life Technologies), and 2200 TapeStation Instrument (Agilent Technologies, Santa Clara, CA, USA) were used to check the concentration, purity, and degradation of extracted genomic DNA. For the next step, samples that passed our quality control thresholds were used.

Genomic DNA (250 ng) from the tissues was sheared by the Covaris S220 (Covaris, Woburn, MA, USA) and used for the construction of the library using customized RNA baits and the SureSelect XT reagent kit, HSQ (Agilent Technologies), according to the manufacturer's protocol. The customized RNA baits covered whole exons and flanking intronic sequences of the 83 genes. After enriched exome libraries were multiplexed, the libraries were sequenced on the HiSeq 2500 sequencing platform (Illumina, USA), as described previously [32]. Briefly, a paired-end DNA sequencing library was prepared through the following processes: genomic DNA shearing, end-repair, A-tailing, paired-end adaptor ligation, and amplification. After the library was hybridized with bait sequences for 16 hours, the captured library was purified and amplified with an index barcode tag. Then, the quality and quantity of the captured library were measured. Sequencing of the exome library was carried out using the 100-bp, paired-end mode of the TruSeq Rapid PE Cluster kit and TruSeq Rapid SBS kit (Illumina, San Diego, CA, USA).

PCR for *ALK* fusion genes

The newly identified glutamine:fructose-6-phosphate transaminase 1 (*GFPT1*)-*ALK* fusion gene was detected by targeted cancer panel sequencing, and its respective genomic rearrangement was confirmed by genomic PCR analysis, followed by Sanger sequencing. Genomic DNA was isolated from formalin-fixed, paraffin-embedded (FFPE) tumor samples using a ReliaPrep FFPE genomic DNA extraction kit (Promega, Madison, WI, USA). The PCR products were indicative of fusion points within intron 18 of *GFPT1* and exon 20 of *ALK*, based on target sequencing results. PCR analysis of genomic DNA for *GFPT1*-*ALK* was performed with a pair of primers flanking the putative fusion point: *GFPT1* F (5'-TCTGTGTGAACTGGCACCTT-3') and *ALK* R (5'-ATTTCAGCCCCTACTACTGCAC-3'). PCR products were then separated on a 2% E-Gel SizeSelect agarose gel (Invitrogen, Carlsbad, CA, USA). For genomic PCR controls, we used DNA from the same FFPE tumor samples with glyceraldehyde-3-phosphate dehydrogenase PCR primers. In reactions that produced a PCR product of the expected size, the amplicons underwent gel purification and sequencing using a 3130 XL ABI Prism sequencer (Applied Biosystems, Foster City, CA, USA) with Bigdye Terminator v3.1 Cycle sequencing kits, according to the manufacturer's instructions.

Supporting Information

S1 Fig. Nucleotide sequence of the glutamine:fructose-6-phosphate transaminase 1 (*GFPT1*)-anaplastic lymphoma kinase (*ALK*) fusion, as determined by Sanger sequencing. (TIF)

S1 Table. Overall Ampliseq results in the entire medullary thyroid cancer (MTC) cohort. (XLS)

S2 Table. Clinical, demographic and pathological characteristics of entire medullary thyroid cancer (MTC) cohort.

(DOCX)

Author Contributions

Conceived and designed the experiments: JMS. Performed the experiments: JHJ YLO MH JWY HWL DK YJ DHK WYP HTS KMK JMS. Analyzed the data: JHJ JWY HWL DK KMK MJA KP JMS. Contributed reagents/materials/analysis tools: YLO JWY DK KMK JMS. Wrote the paper: JHJ JWY JMS. Full access to all of the data in the study and responsibility for the integrity of the data and analysis of the data: JMS. Immunohistochemical assessment: KMK HWL. Review of the manuscript: JHJ YLO MH JWY HWL DK YJ DHK WYP HTS KMK MJA KP JMS.

References

1. Cerrato A, De Falco V, Santoro M. Molecular genetics of medullary thyroid carcinoma: the quest for novel therapeutic targets. *J Mol Endocrinol.* 2009; 43: 143–155. doi: [10.1677/JME-09-0024](https://doi.org/10.1677/JME-09-0024) PMID: [19383830](https://pubmed.ncbi.nlm.nih.gov/19383830/)
2. Goutas N, Vlachodimitropoulos D, Bouka M, Lazaris AC, Nasioulas G, Gazouli M. BRAF and K-RAS mutation in a Greek papillary and medullary thyroid carcinoma cohort. *Anticancer Res.* 2008; 28: 305–308. PMID: [18383861](https://pubmed.ncbi.nlm.nih.gov/18383861/)
3. Elisei R, Cosci B, Romei C, Bottici V, Renzini G, Molinaro E, et al. Prognostic significance of somatic RET oncogene mutations in sporadic medullary thyroid cancer: a 10-year follow-up study. *J Clin Endocrinol Metab.* 2008; 93: 682–687. PMID: [18073307](https://pubmed.ncbi.nlm.nih.gov/18073307/)
4. Arighi E, Borrello MG, Sariola H. RET tyrosine kinase signaling in development and cancer. *Cytokine Growth Factor Rev.* 2005; 16: 441–467. PMID: [15982921](https://pubmed.ncbi.nlm.nih.gov/15982921/)
5. Agrawal N, Jiao Y, Sausen M, Leary R, Bettegowda C, Roberts NJ, et al. Exomic sequencing of medullary thyroid cancer reveals dominant and mutually exclusive oncogenic mutations in RET and RAS. *J Clin Endocrinol Metab.* 2013; 98: E364–369. doi: [10.1210/jc.2012-2703](https://doi.org/10.1210/jc.2012-2703) PMID: [23264394](https://pubmed.ncbi.nlm.nih.gov/23264394/)
6. Donis-Keller H, Dou S, Chi D, Carlson KM, Toshima K, Lairmore TC, et al. Mutations in the RET proto-oncogene are associated with MEN 2A and FMTC. *Hum Mol Genet.* 1993; 2: 851–856. PMID: [8103403](https://pubmed.ncbi.nlm.nih.gov/8103403/)
7. Mulligan LM, Kwok JB, Healey CS, Elsdon MJ, Eng C, Gardner E, et al. Germ-line mutations of the RET proto-oncogene in multiple endocrine neoplasia type 2A. *Nature.* 1993; 363: 458–460. PMID: [8099202](https://pubmed.ncbi.nlm.nih.gov/8099202/)
8. Wells SA Jr., Gosnell JE, Gagel RF, Moley J, Pfister D, Sosa JA, et al. Vandetanib for the treatment of patients with locally advanced or metastatic hereditary medullary thyroid cancer. *J Clin Oncol.* 2010; 28: 767–772. doi: [10.1200/JCO.2009.23.6604](https://doi.org/10.1200/JCO.2009.23.6604) PMID: [20065189](https://pubmed.ncbi.nlm.nih.gov/20065189/)
9. Elisei R, Schlumberger MJ, Muller SP, Schoffski P, Brose MS, Shah MH, et al. Cabozantinib in progressive medullary thyroid cancer. *J Clin Oncol.* 2013; 31: 3639–3646. doi: [10.1200/JCO.2012.48.4659](https://doi.org/10.1200/JCO.2012.48.4659) PMID: [24002501](https://pubmed.ncbi.nlm.nih.gov/24002501/)
10. Shaw AT, Yeap BY, Mino-Kenudson M, Digumarthy SR, Costa DB, Heist RS, et al. Clinical features and outcome of patients with non-small-cell lung cancer who harbor EML4-ALK. *J Clin Oncol.* 2009; 27: 4247–4253. doi: [10.1200/JCO.2009.22.6993](https://doi.org/10.1200/JCO.2009.22.6993) PMID: [19667264](https://pubmed.ncbi.nlm.nih.gov/19667264/)
11. Kwak EL, Bang YJ, Camidge DR, Shaw AT, Solomon B, Maki RG, et al. Anaplastic lymphoma kinase inhibition in non-small-cell lung cancer. *N Engl J Med.* 2010; 363: 1693–1703. doi: [10.1056/NEJMoa1006448](https://doi.org/10.1056/NEJMoa1006448) PMID: [20979469](https://pubmed.ncbi.nlm.nih.gov/20979469/)
12. Shaw AT, Kim DW, Nakagawa K, Seto T, Crino L, Ahn MJ, et al. Crizotinib versus chemotherapy in advanced ALK-positive lung cancer. *N Engl J Med.* 2013; 368: 2385–2394. doi: [10.1056/NEJMoa1214886](https://doi.org/10.1056/NEJMoa1214886) PMID: [23724913](https://pubmed.ncbi.nlm.nih.gov/23724913/)
13. Shaw AT, Engelman JA. Ceritinib in ALK-rearranged non-small-cell lung cancer. *N Engl J Med.* 2014; 370: 2537–2539.
14. Butrynski JE, D'Adamo DR, Hornick JL, Dal Cin P, Antonescu CR, Jhanwar SC, et al. Crizotinib in ALK-rearranged inflammatory myofibroblastic tumor. *N Engl J Med.* 2010; 363: 1727–1733. doi: [10.1056/NEJMoa1007056](https://doi.org/10.1056/NEJMoa1007056) PMID: [20979472](https://pubmed.ncbi.nlm.nih.gov/20979472/)

15. Kelly LM, Barila G, Liu P, Evdokimova VN, Trivedi S, Panebianco F, et al. Identification of the transforming STRN-ALK fusion as a potential therapeutic target in the aggressive forms of thyroid cancer. *Proc Natl Acad Sci U S A*. 2014; 111: 4233–4238. doi: [10.1073/pnas.1321937111](https://doi.org/10.1073/pnas.1321937111) PMID: [24613930](https://pubmed.ncbi.nlm.nih.gov/24613930/)
16. Eng C, Clayton D, Schuffenecker I, Lenoir G, Cote G, Gagel RF, et al. The relationship between specific RET proto-oncogene mutations and disease phenotype in multiple endocrine neoplasia type 2. International RET mutation consortium analysis. *JAMA*. 1996; 276: 1575–1579. PMID: [8918855](https://pubmed.ncbi.nlm.nih.gov/8918855/)
17. Beldjord C, Desclaux-Arramond F, Raffin-Sanson M, Corvol JC, De Keyzer Y, Luton JP, et al. The RET protooncogene in sporadic pheochromocytomas: frequent MEN 2-like mutations and new molecular defects. *J Clin Endocrinol Metab*. 1995; 80: 2063–2068. PMID: [7608256](https://pubmed.ncbi.nlm.nih.gov/7608256/)
18. Sanso GE, Domene HM, Garcia R, Pusiol E, de M, Roque M, et al. Very early detection of RET proto-oncogene mutation is crucial for preventive thyroidectomy in multiple endocrine neoplasia type 2 children: presence of C-cell malignant disease in asymptomatic carriers. *Cancer*. 2002; 94: 323–330. PMID: [11900218](https://pubmed.ncbi.nlm.nih.gov/11900218/)
19. Soda M, Choi YL, Enomoto M, Takada S, Yamashita Y, Ishikawa S, et al. Identification of the transforming EML4-ALK fusion gene in non-small-cell lung cancer. *Nature*. 2007; 448: 561–566. PMID: [17625570](https://pubmed.ncbi.nlm.nih.gov/17625570/)
20. Sasaki T, Rodig SJ, Chirieac LR, Janne PA. The biology and treatment of EML4-ALK non-small cell lung cancer. *Eur J Cancer*. 2010; 46: 1773–1780. doi: [10.1016/j.ejca.2010.04.002](https://doi.org/10.1016/j.ejca.2010.04.002) PMID: [20418096](https://pubmed.ncbi.nlm.nih.gov/20418096/)
21. Girard N. Crizotinib in ALK-positive lung cancer. *Lancet Oncol*. 2012; 13: 962–963. doi: [10.1016/S1470-2045\(12\)70375-3](https://doi.org/10.1016/S1470-2045(12)70375-3) PMID: [22954506](https://pubmed.ncbi.nlm.nih.gov/22954506/)
22. Gadgeel SM, Gandhi L, Riely GJ, Chiappori AA, West HL, Azada MC, et al. Safety and activity of alectinib against systemic disease and brain metastases in patients with crizotinib-resistant ALK-rearranged non-small-cell lung cancer (AF-002JG): results from the dose-finding portion of a phase 1/2 study. *Lancet Oncol*. 2014; 15: 1119–1128. doi: [10.1016/S1470-2045\(14\)70362-6](https://doi.org/10.1016/S1470-2045(14)70362-6) PMID: [25153538](https://pubmed.ncbi.nlm.nih.gov/25153538/)
23. Senderek J, Muller JS, Dusl M, Strom TM, Guergueltcheva V, Diepolder I, et al. Hexosamine biosynthetic pathway mutations cause neuromuscular transmission defect. *Am J Hum Genet*. 2011; 88: 162–172. doi: [10.1016/j.ajhg.2011.01.008](https://doi.org/10.1016/j.ajhg.2011.01.008) PMID: [21310273](https://pubmed.ncbi.nlm.nih.gov/21310273/)
24. Wong DW, Leung EL, Wong SK, Tin VP, Sihoe AD, Cheng LC, et al. A novel KIF5B-ALK variant in non-small cell lung cancer. *Cancer*. 2011; 117: 2709–2718. doi: [10.1002/cncr.25843](https://doi.org/10.1002/cncr.25843) PMID: [21656749](https://pubmed.ncbi.nlm.nih.gov/21656749/)
25. Ou SH, Klempner SJ, Greenbowe JR, Azada M, Schrock AB, Ali SM, et al. Identification of a novel HIP1-ALK fusion variant in Non-Small-Cell Lung Cancer (NSCLC) and discovery of ALK I1171 (I1171N/S) mutations in two ALK-rearranged NSCLC patients with resistance to Alectinib. *J Thorac Oncol*. 2014; 9: 1821–1825. doi: [10.1097/JTO.0000000000000368](https://doi.org/10.1097/JTO.0000000000000368) PMID: [25393796](https://pubmed.ncbi.nlm.nih.gov/25393796/)
26. Sasaki T, Okuda K, Zheng W, Butrynski J, Capelletti M, Wang L, et al. The neuroblastoma-associated F1174L ALK mutation causes resistance to an ALK kinase inhibitor in ALK-translocated cancers. *Cancer Res*. 2010; 70: 10038–10043. doi: [10.1158/0008-5472.CAN-10-2956](https://doi.org/10.1158/0008-5472.CAN-10-2956) PMID: [21030459](https://pubmed.ncbi.nlm.nih.gov/21030459/)
27. Morris SW, Kirstein MN, Valentine MB, Dittmer K, Shapiro DN, Look AT, et al. Fusion of a kinase gene, ALK, to a nucleolar protein gene, NPM, in non-Hodgkin's lymphoma. *Science*. 1995; 267: 316–317.
28. Ma Z, Cools J, Marynen P, Cui X, Siebert R, Gesk S, et al. Inv(2)(p23q35) in anaplastic large-cell lymphoma induces constitutive anaplastic lymphoma kinase (ALK) tyrosine kinase activation by fusion to ATIC, an enzyme involved in purine nucleotide biosynthesis. *Blood*. 2000; 95: 2144–2149. PMID: [10706887](https://pubmed.ncbi.nlm.nih.gov/10706887/)
29. Simbolo M, Mian C, Barollo S, Fassan M, Mafficini A, Neves D, et al. High-throughput mutation profiling improves diagnostic stratification of sporadic medullary thyroid carcinomas. *Virchows Arch*. 2014; 465: 73–78. doi: [10.1007/s00428-014-1589-3](https://doi.org/10.1007/s00428-014-1589-3) PMID: [24828033](https://pubmed.ncbi.nlm.nih.gov/24828033/)
30. Roy S, Durso MB, Wald A, Nikiforov YE, Nikiforova MN. SeqReporter: automating next-generation sequencing result interpretation and reporting workflow in a clinical laboratory. *J Mol Diagn*. 2014; 16: 11–22. doi: [10.1016/j.jmoldx.2013.08.005](https://doi.org/10.1016/j.jmoldx.2013.08.005) PMID: [24220144](https://pubmed.ncbi.nlm.nih.gov/24220144/)
31. Paik JH, Choe G, Kim H, Choe JY, Lee HJ, Lee CT, et al. Screening of anaplastic lymphoma kinase rearrangement by immunohistochemistry in non-small cell lung cancer: correlation with fluorescence in situ hybridization. *J Thorac Oncol*. 2011; 6: 466–472. doi: [10.1097/JTO.0b013e31820b82e8](https://doi.org/10.1097/JTO.0b013e31820b82e8) PMID: [21258247](https://pubmed.ncbi.nlm.nih.gov/21258247/)
32. Lee YS, Cho YS, Lee GK, Lee S, Kim YW, Jho S, et al. Genomic profile analysis of diffuse-type gastric cancers. *Genome Biol*. 2014; 15: R55. doi: [10.1186/gb-2014-15-4-r55](https://doi.org/10.1186/gb-2014-15-4-r55) PMID: [24690483](https://pubmed.ncbi.nlm.nih.gov/24690483/)